EFFECT OF FREEZING RATE AND COMPOSITION CHANGES ON THE PREFERRED GROWTH DIRECTION OF DIRECTIONALLY SOLIDIFED Sn-Bi ALLOYS

By

Anil Kumar

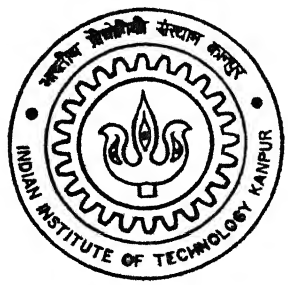

DEPARTMENT OF MATERIALS AND METALLURGIACAL ENGINEERING

Indian Institute of Technology Kanpur

JULY, 2003

EFFECT OF FREEZING RATE AND COMPOSITION CHANGES ON THE PREFERRED GROWTH DIRECTION OF DIRECTIONALLY SOLIDIFED Sn-Bi ALLOYS

A Thesis Submitted

in Partial Fulfillment of the requirements

for the degree of

MASTER OF TECHNOLOGY

BY

Anil Kumar

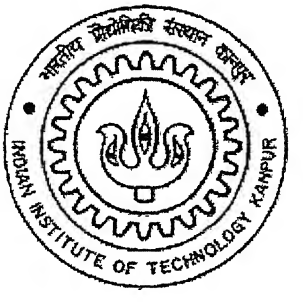

DEPARTMENT OF MATERIALS AND METALLURGICAL ENGINEERING

INDIAN INSTITUTE OF TECHNOLOGY, KANPUR

JULY, 2003

CERTIFICATE

This is to certify that the work contained in this thesis entitled, **"Effect of Freezing Rate and Composition Changes on the Preferred Growth Direction of Directionally Solidified Sn-Bi Alloys"**, by Anil Kumar has been carried out under our supervision and that it has not been submitted elsewhere for a degree.

Jitendra Kumar
(Jitendra Kumar)
Professor
Materials Science Programme
Indian Institute of Technology
Kanpur - 208016

(V. Bansal)
Professor
Department of Materials and
Metallurgical Engineering
Indian Institute of Technology
Kanpur - 208016

Acknowledge

I wish to express my sincerity and deep sense of gratitude to Dr. V. Bansal, Professor, Department of Materials and Metallurgical Engineering and Dr. Jitendra Kumar, Professor, Materials Science Programme, I.I.T. Kanpur for their valuable guidance and constant encouragement throughout the course of this work. I also express my hearty gratitude to Dr. M. Mangole, Mr. Uma shankar Singh, Mr. G. S. Thapaa, Mr. B. D. Tripathi, Mr. Indra Pal Singh, Ruchi, Prita, Swaraj, Mamta, Pranay Kumar, Ranjan Upadhyay, K.V. Arya, Amitesh, and others who helped in preparing this thesis.

July, 2003. Anil Kumar

CONTENTS

LIST OF TABLES

LIST OF FIGURES

ABSTRACT

Effects of freezing rate and composition changes on the preferred growth direction of the directionally solidified Sn-Bi alloys, belonging to body centred tetragonal structure, have been studied by Laue X-ray back reflection method. For this, Sn-Bi alloys of composition 2wt% and 6wt%Bi, directionally solidified at freezing rates of 51.02 μm/s, 68.39 μm/s, and 127.3 μm/s, have been electropolished and subjected to microstructural examination for locating the largest grain before recording their Laue back reflection photographs For indexing of Laue spots and determining the possible zone axes, use is made of (i) their x-y coordinates, (ii) their angular distances readings on Greninger chart, (iii) stereographic projections, and (iv) a computer program. At low freezing rates, 2wt%Bi alloys have been shown to grow preferentially along [1 $\bar{1}$ 0] and/or [1 1 0]. The direction, however, deviates at high freezing rate to [$\bar{2}$ 1 3]. The deviation is attributed to (i) the diversion of the free energy available in creating large interface and (ii) the appearance of serrations in the flanges of the cross section of the cells at higher freezing rates. The effect of changes in composition is shown to give rise to altogether different growth direction in Sn-Bi alloys. While in 2wt%Bi alloy, growth occurs along [1 $\bar{1}$ 0], the corresponding direction in 6wt%Bi is [0 1 $\bar{1}$]. This deviation is possibly caused by occurrence of constitutional supercooling at higher Bi content leading to protrusion at the interface that may cap the growing crystal.

CHAPTER 1

INTRODUCTION

Change of phase from liquid to solid is called solidification. We are considering a system, which is directionally solidified. In this, heat is extracted from one end and solidification proceeds from there to the other end. In the process, solid-liquid interface moves in the melt. The stability of the interface depends upon various parameters, such as growth rate, degree of undercooling, composition, temperature gradient, etc. The nature of interface determines whether the resulting solid is a single crystal or polycrystal. For a single crystal, the stability of the interface is maintained throughout the solidification process without any perturbation. Once the interface stability gets disturbed, this is characterized by the columnar structure.

The importance of directional solidification in the system to get the desired properties like magnetic properties, composite properties, creep strength, texture, etc. It is applicable to metals, alloys, organic materials and other systems also. Zone refining, which is the method of purification of impure metals in which impure metal rod heated from one end and subsequent cooling is carried out is an example of directional solidification

The movement of stable and planer solid-liquid interface during directional solidification produced single crystal for computer chips and solar cells. Further, perfectly aligned laminated composite structures have been formed through directional solidification with superior properties such as high strength, durability and reliable performance at high temperature applications, etc. Turbine blades with vastly improved properties and magnetically soft materials with high magnetic permeability have also been made with directional solidification techniques [1].

The present work involves finding out the preferred crystallographic growth directions in directionally solidified Sn-Bi alloys (which usually have a body centered tetragonal structure) by Laue back reflection method. It essentially requires indexing and

identification of spots and zone(s) recorded on the Laue photograph. Indexing procedures are, however, straight forward and easier for cubic and hexagonal closed packed (h.c.p.) systems, since the tables of interplanar angles and standard stereographic projections are available. For other systems, indexing of Laue pattern is difficult and time consuming as tables of interplanar angles and standard stereographic projections are not available. So various approaches have been suggested to index the Laue patterns by employing a computer [2].

Directionally solidified alloys of Sn-Bi alloys show dendritic structure. The primary dendrites are plate shaped and nearly parallel to the growth direction, which, in turn, is the ingot axis itself. It is known [3-5] that the growth directions in pure tin and Sn-12wt%Bi alloys are generally [110], [1 $\bar{1}$ 0] and sometime [001] as well. Secondary arms grow in [1 $\bar{1}$ $\bar{1}$] and [$\bar{1}$ 1 $\bar{1}$] directions; these are perpendicular to the [110] direction and are 138^0 apart, respectively. Secondary arms in <111> directions are found only on one side of primary dendrite i.e. secondary arms do not grow along [$\bar{1}$ 11], [1 $\bar{1}$ 1] or [111] directions. The reason being their relatively small angles to the primary dendrite or other secondary arms [4]. The growth direction varies with composition and solidification rate. Our aim is to compare the orientation reported in literature to the orientation obtained in this work.

Ingots of tin alloys with 2wt% and 6wt% bismuth, prepared earlier by directional solidification process at different freezing rates, were sectioned longitudinally as well as transversely and polished manually. Finally, the surface was electrolytically polished in a specifically developed cell. The samples were then exposed to white X-ray radiation from a copper target and back reflection Laue pattern recorded for each sample. Also they were microscopically examined under a metallurgical microscope.

Angular distance of the spots of Laue patterns was measured with the help of the Greninger chart. Which transfer on the Wulff net for stereographic projection of the spots. Further, replicas of films are made on transparent graph papers, which are helpful to measure the coordinate of the spots assuming center of the hole made in the films as origin. These are the input data for computer program. Indexing of the spots was carried out. Also,

the computer programming has been written in 'C' language [6] and which assigns indices to spots as well as to the zone axis. The orientation of the crystal can be easily determined after assigning indices to the spots and zone axes

CHAPTER 2

LITERATURE SURVEY

Sn-Bi alloys are used in soldering. The equilibrium phase diagram of Sn-Bi alloy is shown in Fig. 2.1 [7]. Maximum solid solubility of Bi in Sn is 21 wt% and eutectic composition corresponds to 57[illegible] The eutectic temperature of this system is 139 ^{0} C. Maximum solid solubility of Sn in Bi is 0.1 wt%. These alloys are candidates for lead free (i) soldering material for semiconductor packages and (ii) stable plating solution even at high current density. Sn-Bi solder pastes with variable melting points have been developed. These exhibit good solder ball formation under reflow conditions, intermetallic reactions with pad surface comparable to that of Pb-Sn eutectic and no evidence of Pb-Sn-Bi ternary alloy formation with lead contamination. Directional solidification/freezing also has direct relevance to certain commercial process, such as production of turbine blades; growing of single crystal etc. The process is also called the Bridgman technique. In this, specimen melt is moved from a furnace (Fig. 2 2) into a cooling device through an isolated region of high thermal gradient. The isotherm in the insulated section is closely spaced and this facilitates control of the interface position. Furthermore, curvature of the isotherm is often very small and the growth front is essentially planar in nature, lying perpendicular to the furnace axis.

Trivedi et. al [8] carried out the directional solidification studies in the pivalic acid-ethanol system in which significant anisotropies present in the interface kinetics and the interfacial free energy. These anisotropic characteristics influence the microstructure and often lead to the formation of dendrite and cells, which are tilted with respect to the heat flow direction. The dendrites are always formed in the preferred crystallographic direction, while the angle of tilt for cells is governed by nature of heat flow and the anisotropy.

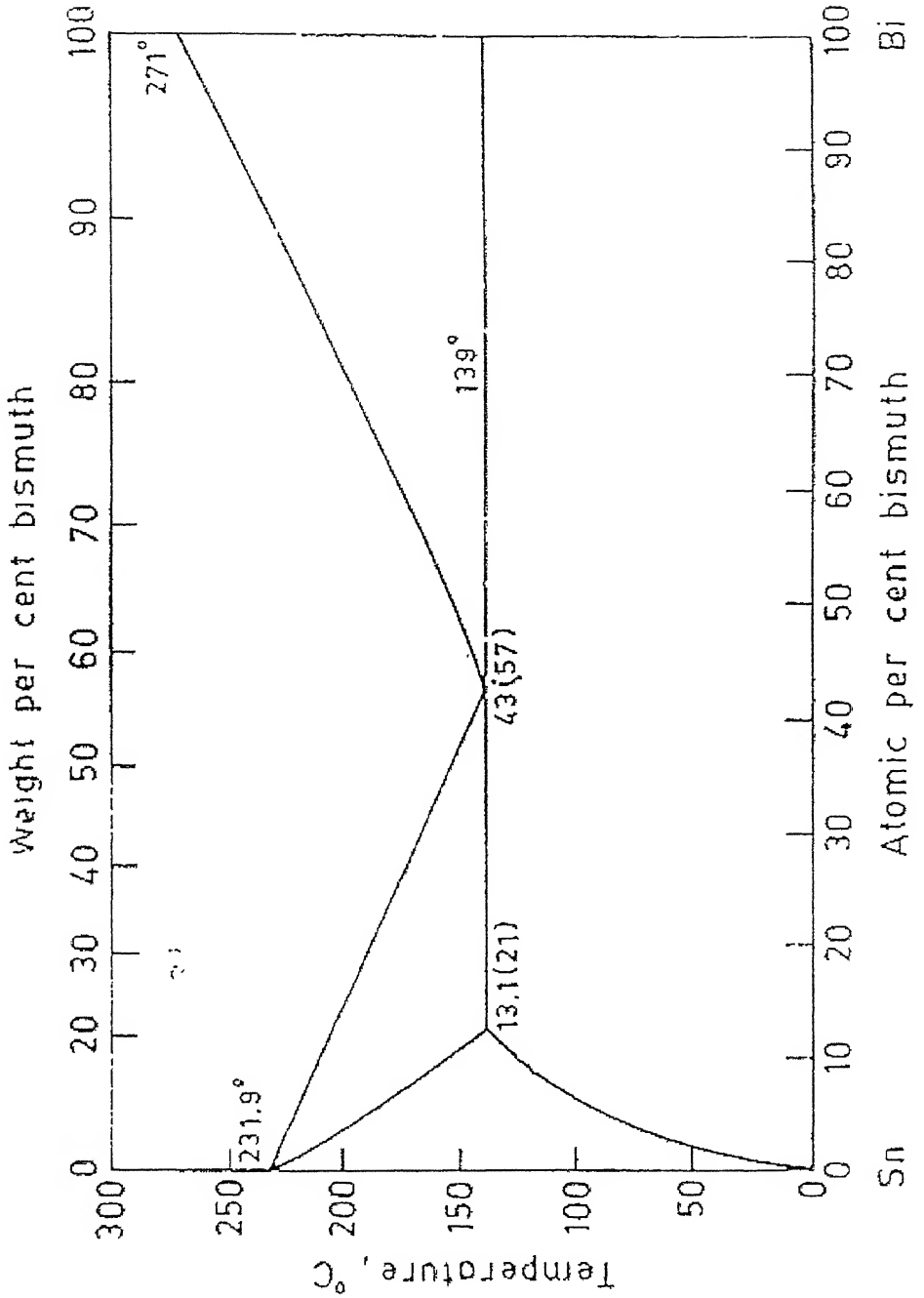

Figure 2.1 Sn-Bi equilibrium diagram at eutectic temperature (139^0), composition given in brackets corresponds to weight % of bismuth.

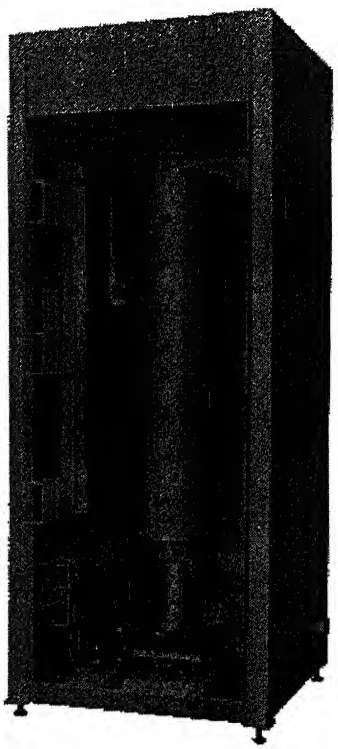

Fig. 2.2 Bridgman Vertical Furnace

Further, this tilt angle increases with the velocity and becomes maximum when the cell growth direction coincides with the preferred growth direction, i.e., <001> for the cubic pivalic acid crystals. At this point, the transition from cellular to dendritic morphology occurs. The cellular spacing as well as the amplitude of cells is found to alter significantly with the angle of tilt under identical conditions of growth rate, temperature gradient, and composition The cell-dendrite transition occurs when the anisotropic effects dominate and results in the growth of dendrites in the preferred growth direction.

Larrea et. al. [9] studied the microstructure and crystallographic orientation relationship of directionally solidified CaF_2–MgO eutectics obtained by the Bridgman technique. The samples contained single crystal MgO fibers (~1.4 μm length and spacing ~ 8 μm) oriented parallel to the cubic axis of a CaF_2 matrix. The fracture toughness was shown to improve through crack deflection at the interface.

Martorano and Capochi [10] studied the effect of freezing rate on the microsegreration of directionally cast samples of Cu-8 wt pct Sn alloys. They found microsegregation to be more at the centre and less at the surface of the ingot, because of existence of lower cooling rate at the centre than at the surface. Obviously, there was less time available for solute atoms to diffuse near the surface due to prevailing high cooling rate.

Laue back reflection method is quite accurate and convenient for determining the orientation of the single crystal or individual grain of an aggregate. In this, it is necessary to assign the indices to diffraction spots lying on a particular curve in the Laue back reflection photograph. Spots fall on hyperbolas when ϕ (angle between the transmitted beam and the zone axis) lies between 45^0 and 90^0 or 90^0 and 135^0. At $\phi=90^0$, loci of spots correspond to straight lines[11].

Indexing of Laue spots in case of cubic and hexagonal closed packed system is straight forward as tables of interplanar angles and stereographic projections are available. But for other system, it is tedious and time consuming. So attempt was made to index the pattern using a computer

Hung et al. [2] and Christensen et al. [12] developed computer algorithms in FORTRAN language for the rapid solution of Laue back reflection patterns of cubic crystals The computational scheme compares the angles measured with reflections recorded on the Laue patterns and actual interplanar angles of the system. Any film to specimen distance may be used. The algorithm duplicates the traditional technique of matching the angles between prominent reflections on the film with the true values of interplanar angles. The program seeks a solution by assigning trial indices to a pair of reflections, generating the function of the true interplanar angles and comparing with the data obtained from the Laue pattern. The error setting for this program was ± 2 degree. They restricted their search from (3 3 3) to $(\bar{3}\,\bar{3}\,\bar{3})$. If the error lies within allowable error limit then the program generates the indices of the Laue spots.

Camp and Clum [13] have attempted to index the Laue back reflection pattern of a zinc crystal (hexagonal structure with c/a ratio as 1.856) by (i) writing a digital computer program for generating a table of interplanar angles for an arbitrary crystal structure and (ii) undertaking systematically search to obtain a consistent fit with the Laue back reflection data. The program was originally written in ALGOL version and then in FORTRAN II and IV. There was option to obtain the Greninger-chart coordinates γ and δ for each pole as well.

Cornelius [14] produced a simple computer program in FORTRAN IV for the simulation and analysis (both position and intensity) of Laue back reflection photographs for a single crystal with any crystal system and orientation. The input data consist of X-ray tube voltage, specimen-film distance, maximum spot-to-centre distance, lattice parameters, ranges for Miller indices, possible crystal orientation and atomic number with position in the unit cell.

Laugier [15] made an interactive FORTRAN IV program, which allow the orientation matrix of a crystal to be determined and refined without ambiguity, from a transmission or reflection Laue photographs. The indexing method adopted was that of Riquet and Bonnet [16]. With the unit cell dimensions known, the knowledge of the

coordinates (both in the crystal and in experimental frames of reference) of two or more reciprocal points is enough to find the orientation matrix of the crystal. Thus, the problem reduces to indexing of reflection of the Laue pattern and checking that the solution obtained is correct. This interactive program needs a graphics screen with plotter as optional. The input data is simply the coordinates of n Bragg spots on the Laue photograph. The indexing procedure start with two reflections, which are at the intersection of zonal planes and thus have small Miller indices. The angle between the corresponding scattering vectors is compared within a given angular tolerance to the angle between all possible pairs of reciprocal vectors up to a given limit of the Miller indices.

Haskell et. al. [17] have written an algorithm in BASIC for a minicomputer for indexing of asymmetrical/symmetrical transmission or back reflection Laue patterns of any system and used least square method for determining the crystallographic directions. Zones with indices as high as eight and spots with Miller indices as high as 24 have been identified in back reflection photograph of echinoid calcite.

Kumar and Bansal [18] have developed a method based on a computer program in FORTRAN 77 to index the Laue back reflection pattern for a body centred tetragonal system. Coordinates of the Bragg spots, lattice parameters, and film to specimen distance form the input of the program. The program generates the set in indices and calculates the angle ϕ_T between the pair of indices. This way a table giving angles between pair of indices is produced for the system under study. The program search the indices between $(\bar{6}\,\bar{6}\,\bar{6})$ and (6 6 6). The experimental angles (ϕ_E) determined from the coordinates of Laue spots are matched with (ϕ_T) for identifying the possible indices. The error limit set was ± 3 degrees. If the difference between ϕ_T and ϕ_E lie within this limit, the program assigns the indices to various spots and subsequently calculates the zone axis also. Kumar and Bansal [18] studied directionally solidified Sn-6wt%Bi alloy by Laue back reflection and found the primary growth direction 27^0 away from [11 0].

Ranjan [6] developed a computer code in 'C' language for indexing of Laue back reflection (LBR) pattern for a body centred tetragonal system and investigated directionally solidified Sn-2wt%Bi alloys. The input data include lattice parameters, coordinates of the Laue spots, and film to specimen distance. They also restricted their search between $(\bar{6}\ \bar{6}\ \bar{6})$ and (6 6 6) and set the error limit of ± 3 degrees between ϕ_T and ϕ_E. He found the primary growth direction 46 to 48 degrees away from [1 1 0], 46 to 76 degrees away from [1 $\bar{1}$ 0], and 40 to 58 degrees away from [0 0 1]

Bolling, Kramer, and. Tiller [5] have studied the directionally solidified Sn-Bi alloys and found the dendrite growth along the preferred direction [1 1 0].

Aheran and Flemings [4] have investigated the dendrite morphology of unidirectional Sn-12wt%Bi alloys and found columnar growth of primary arms along [1 1 0] direction. The secondary dendrite arms, however, grow along [1 $\bar{1}$ $\bar{1}$], [$\bar{1}$ 1 $\bar{1}$] and [1 1 2] directions. The first two directions viz., [1 $\bar{1}$ $\bar{1}$] and [$\bar{1}$ 1 $\bar{1}$] are perpendicular to primary growth direction [1 1 0] and are 138 degrees apart. Further, they found no evidence of secondary arms growing in the direction [$\bar{1}$ 1 1], [1 $\bar{1}$ 1], or [1 1 1].

Weinberg and Chalmers [3] studied the dendrite growth in 99.98% pure single crystal of tin. The 'c' axis lies in the horizontal plane of the specimen and perpendicular to general direction of solidification. The 'a' and 'b' axes lie at 45 degree to this horizontal plane. They found a number of dendrite rows growing parallel to the direction of solidification with large vertical secondary branches

Chandrashekhar and Veal [19] have produced tables of angles between planes and zone axes for β-tin and indium having body centred tetragonal structure with c/a ratio as 0.54554 and 1.07586, respectively to aid indexing of spots on a Laue photograph. Similarly, Frounfelker and Hirthe [20] have used a computer program to generate tables of angles between planes for tetragonal systems in general with c/a lying in the range 0.05–2.00 in steps of 0.05 and β-tin, SnO_2 and Pb_3O_4 and TeO_2 in particular.

Lee and Raynor [21] reported the variation of lattice parameters of Sn-Bi alloys. Accordingly, c/a ratio varies from 0.5455 for pure tin to 0.5451 for 6wt% Bi in tin

CHAPTER 3

EXPERIMENTAL SET UP AND PROCEDURE

3.1 INTRODUCTION

The objective is to find out the preferred growth direction in Sn-Bi alloys of composition 2-6 wt% Bi (Table 3.1), which have been directionally solidified at different rate of freezing. The experimental work can be divided into three sections viz.,

(1) samples preparation,
(2) recording of Laue patterns, and
(3) obtaining input data for further analysis.

3.2 SAMPLES PREPARATION

The cylindrical (dia ~11 mm and 30-35 mm) samples of Sn-Bi alloys directionally solidified earlier by Kumar and Das [22, 23] were taken. Transverse section of each was first polished on belt grinder and then turned by 90^0 for the subsequent polishing with emery paper 1/0 – 4/0. With change of emery paper grade, samples were rotated every time by 90^0. The polished surface was then subjected to mechanical polishing using cloth wheel with MgO slurry or electropolishing. Since the alloys were very soft, due care was taken during cloth polishing. But, in mechanical polishing surface gets somewhat strained Hence, electrolytic polishing was preferred. Some portion of the sample (not required to be polished) was covered with Goodlass nerolac varnish. The procedure used for electropolishing is discussed in the next section. The polished samples were etched in a solution consisting of 1 g of $K_2Cr_2O_7$, 7 ml. of conc. HCl and 86 ml. of distilled water. The microstructure was observed in a metallurgical microscope to locate the large grain for incident X-ray beam to strike that grain only for obtaining the back reflection Laue photograph.

3.2.1 Electrolytic polishing set up

The schematic diagram of the electropolishing set up is shown in the Fig. 3.1. An L-shaped cathode made of tin held and partly covered by glass was used. It consists of plate of dimension 30 mm x 20 mm x 8 mm brazed at the middle of the shorter edge to a tin rod of diameter 3 mm and length 20 cm A hollow cylindrical sample holder was made of teflone with three threaded holes, two radially and one from the top (Fig 3.2). Two holes on the side are used to tighten the sample in the holder against the teflon sample support (Fig 3.2b) with screws. A teflon rod with axial hole and external threads (Fig 3.3b) is used to hold the sample holder (Fig 3.3a). The brass holder has three radial screws in the lower portion to hold the teflon rod (Fig 3.3b). A hollow brass tube is brazed to the brass holder on its top. Teflone is used for making holder because it does not react with the electrolyte.

The electrolyte is put in a glass tank. A magnetic stirrer is used to continuously stir electrolyte to prevent the localized building of concentration. Electropolishing removes points and projections from metal surface. It is a non-mechanical process and referred to as a "reverse plating" process. Temperature of the electrolyte is also maintained. The current-voltage (I-V) characteristic curve of the set up shows a plateau (constant current in a voltage range) and defines the electropolishing conditions of the system Voltage is generally chosen at the middle of plateau region. The part of the sample, which is not to be electropolished , is covered with a varnish.

For electrical connection the cathode made of tin is connected to the negative terminal of CVCC power supply source (APLAB) Regulated DC Power Supply; 70V, 6A). A copper wire was passed through the brass tube and teflone holder. This wire extends to the sample holder and is brazed to the silver sheet there. The silver sheet touches the sample and lies in between the sample and supporting teflone blank. The top end of the copper wire is connected to the positive terminal of the power supply.

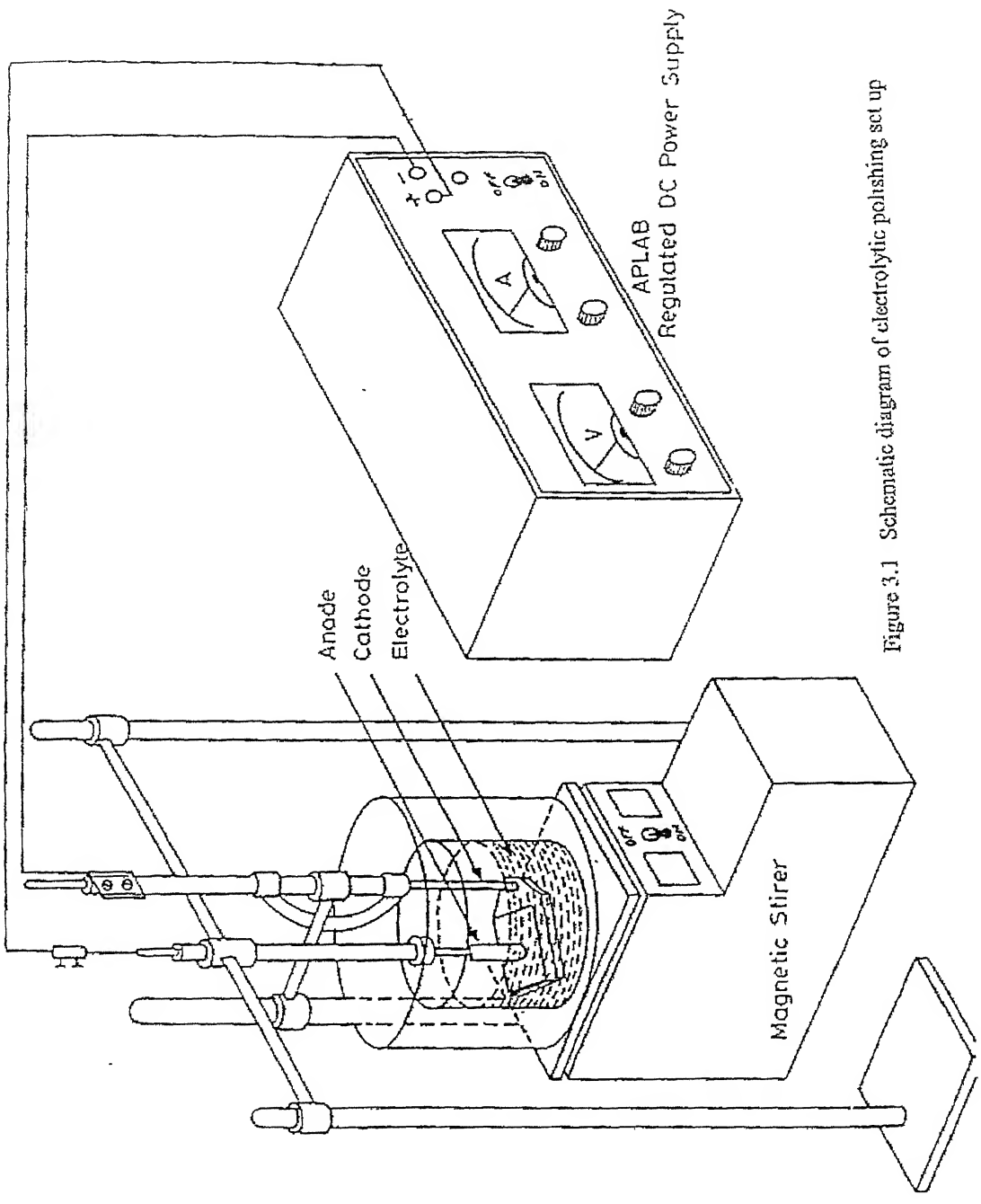

Figure 3.1 Schematic diagram of electrolytic polishing set up

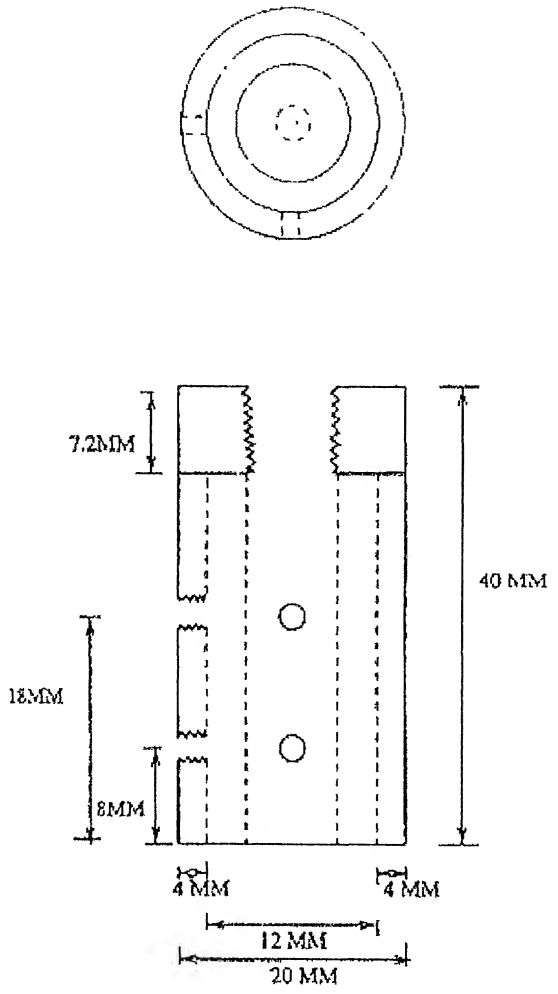

Figure 3.2a Teflon sample holder.

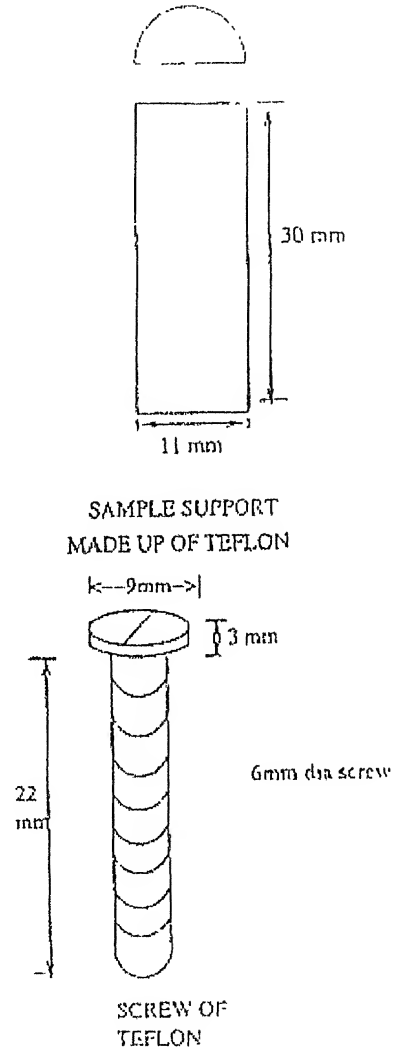

Figure 3.2b Teflon screw and Teflon support.

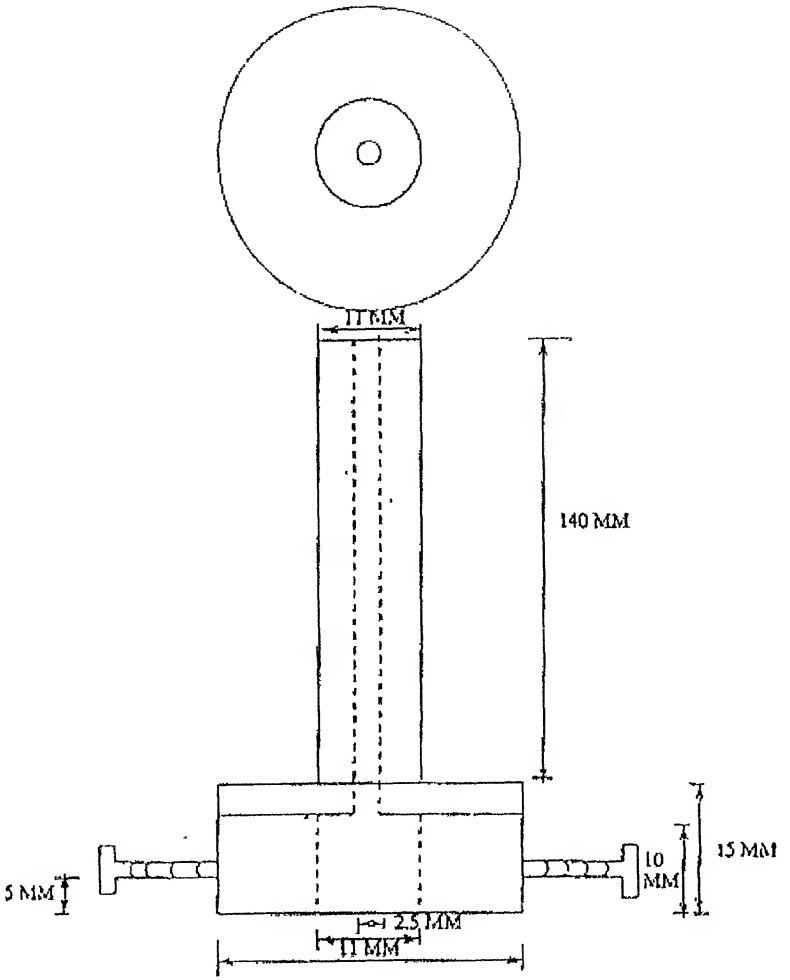

Figure 3.3a Brass holder to hold Teflon sample holder.

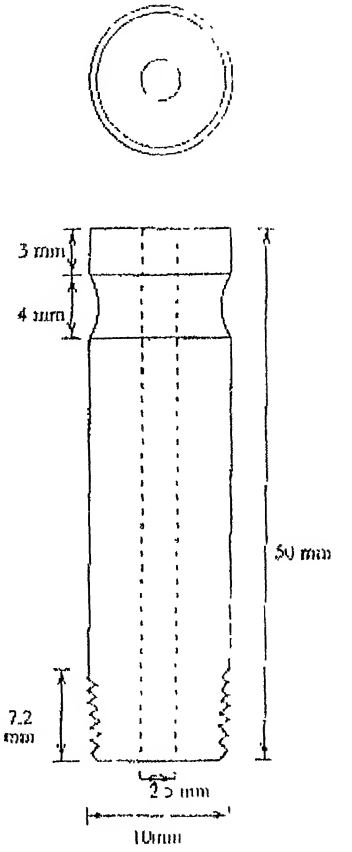

Figure 3.3b Threaded Teflon rod to hold sample holder

3.2.2 Electrolyte preparation

Electrolyte consists of different chemical reagents It is prepared very carefully as some of reagents are hazardous for skin. Electrolyte used for polishing of tin and its alloys [24,25] contained 70% (v) ethanol (absolute), 12% (v) distilled water, 10% (v) 2-butoxyethanol and 8% (v) perchloric acid (70%) of specific gravity 1.67 It is prepared by first mixing distilled water and ethanol [26]. Since perchloric acid is hazardous, it is added to water and ethanol solution cautiously. 2-butoxyethanol (butyl cellosolve) is added to the above solution immediately before use. The solution has an oily appearance. After 4-5 days, white precipitate is formed in the electrolyte, which gets settled at the bottom and gives awful smell.

3.2.3 Electrolytic polishing

The electrolytic polishing set up is shown in the Fig. 3.1. With increase in voltage by coarse regulator of the source (CVCC 0-70 V, 6 A), current values were noted down with stirring and without stirring conditions at 20 seconds interval. Temperature of the electrolyte is maintained at 18°C by placing the tank in ice bath and measured by a thermometer. The observed values are listed in Table 3.2. The I-V characteristics are shown in Fig. 3.4. Clearly, the current first increases with voltage and becomes constant for certain range and increase afterwards. Thus, the I-V curve can be considered to have three stages. In stage I, current increases, stage II corresponding to plateau region, and stage III begins when current increases again. In stage I sharp points or projections on the surface of sample gets removed by etching process. Polishing occurs in the plateau region. In stage III, pits are formed. Voltage is, therefore, set at the middle of plateau for polishing In general, for tin and its alloys, current density of about 3.90 ampere per square centimeter and time of 20 seconds are required for the prefinished sample with 3/0 emery paper [25] In the present case, continuous stirring condition was used for polishing the sample at a voltage of 34 V and current 1.39 A for 20 seconds. This corresponds to a current density of about 3.5 ampere per square centimeter.

Table 3.1 Composition and freezing Rate of Samples

Sample No.	Composition (wt%)	Freezing rate (μm/sec)
1	2	127.30
2	2	68.39
3	6	68.39
4	2	51.02

TABLE 3.2 Voltage and Current

Voltage (Volt)	Current (A)	
	With stirring	Without stirring
10	0.17	-
12	0.27	-
14	0.39	-
16	0.44	-
18	0.50	-
20	0.58	0.44
22	0.69	0.51
24	0.77	0.60
26	0.89	0.65
28	1.35	0.85
30	1.38	0.85
32	1.39	0.87
34	1.39	0.88
36	1.39	0.88
38	1.41	0.89
40	1.65	1.00
42	1.93	1.20
44	2.20	1.60

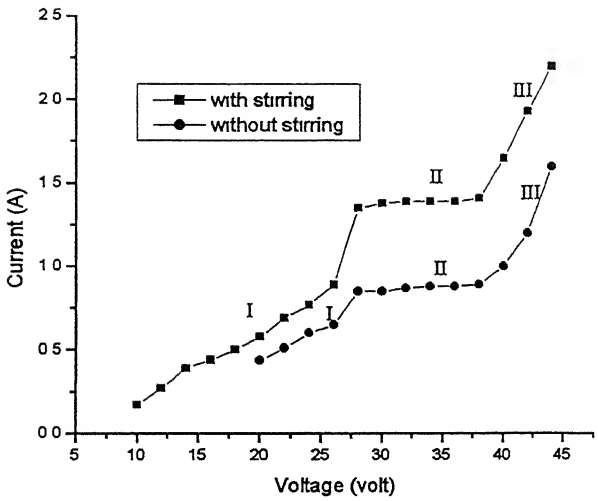

Figure 3.4 I – V characteristic curve at 18^0C

3.2.4 Microstructure observation

The purpose of microstructure observation in transverse section is to locate the large grains for exposing to X-ray beam. Samples were etched in $K_2Cr_2O_7$ solution consisting of 1 g $K_2Cr_2O_7$, 7 ml. of conc. HCl and 86 ml of distilled water. The microstructure was observed in a metallurgical microscope at 50X magnification. The large grains were identified and marked X-ray beams are focused on the located grain.

3.3 Recording of Laue back reflection pattern

Samples were then repolished and exposed to continuous X-ray radiation. The photographic film was cut in size of 98 mm x 81 mm and placed in a cassette. Right top corner of the film was cut for identification and noting the mounting condition while viewing from the specimen side. It then indicates the face on which diffracted X-ray beam strikes. The film was wrapped in a black envelope to protect it from visible light. Punching at the centre of the film was done to allow X-ray beam to pass through and strike the sample. Film to specimen distance is kept at 3 cm. Collimator is inserted in the hole made in film. Samples were screwed in a brass holder, which, in turn, was fixed in the stand in front of collimator. It was ensured that the size of the grain chosen should not be less than diameter of the incident X-ray beam. If it is not so, then the spots formed on the film due to two or more grains and the interpretation becomes difficult. Samples were exposed to 12 hours. X-ray films were developed and washed in a usual way. The films were dried at room temperature. The Laue photograph was then ready for further analysis/interpretation.

3.4 Measurements of x and y coordinates of Laue spots

For obtaining x and y coordinate of spots, the Laue back reflection pattern is kept on a glass plate and a transparent graph paper of 1.0 mm. division fixed over the film in such a way that the cut corner lay to the left top. By illuminating the glass plate Laue spots are clearly seen and their traces are made on the transparent graph paper. Subsequently, x and

y-axes are marked on the paper with the origin at the centre of the hole in the film. Positive x-axis goes to the left and the positive y-axis goes up. Thus, a replica of the film is prepared. The x and y coordinates of each spot are measured with accuracy of ± 0.2 mm and noted in the logbook.

3.5 Identification of zones

For identification of zones to which the Laue spots belong, stereographic projection was drawn for each case. For this, the angular distances γ and δ are measured with the help of Greninger chart for specimen to film distance of 3 cm. Greninger chart is placed over the film in such a way that the top cut corner lies on the left upper half. The angles γ and δ, read from the chart, are then laid out on the stereographic projection. The underlying Wulff net oriented so that its meridians run from side to side, not top to bottom The reason for this is the fact that diffraction spots which lie on curves of constant γ come from planes of a zone, and the poles of these planes must therefore lie on a great circle on the projection. The γ, δ coordinates corresponding to diffraction spots on the lower half of the film are obtained simply by reversing the Greninger chart end for end The spots belonging to one great circle are located and all possible great circles are traced, with each great circle containing minimum of three spots. The spots belonging to one great circle are known as spots of one zone. The great circle containing large number of spots is considered as low indexed zone. At least two zones are located in each Laue pattern. The point lying at the intersection of two or more zones are considered as the prominent spot of low indices.

After selecting few important zones, the zone axes are located on the stereographic projection at 90^0 away. After locating zone axes on the stereographic projection, the angle between the zones is measured by bringing the corresponding points on a particular great circle of the Wulff net.

Proper selection of the desired number of spots is important for indexing. The spots are numbered arbitrarily in the beginning and marked in the stereographic projection. A

minimum of five or six spots belonging to two/three zones is selected for further work in each case.

At the point of intersection of zones, tangents are drawn on each curve. Angles are then measured between the tangents. These are the angles between the chosen zones

3.6 Determination of growth direction

The computer programming gives the indices of spots and possible zone axes. The orientation of the grain can then be determined easily. In tin-bismuth alloys, primary dendrites are nearly parallel to the growth direction. The reported growth direction are [1 1 0], [1 $\bar{1}$ 0] and [0 0 1]. Angle between the indexed zone and [1 1 0] is calculated. Stereographic projection of the pattern is fixed over the Wulff net in such a manner that x and y axes of the projection coincide with the W-E and N-S direction of the Wulff net. The pole of one of the zone axis is first rotated with respect to N-S axis to bring the pole on the circumference of the net. The angle by which the pole gets rotated is noted down (say θ). The projection is again rotated about the centre of the Wulff net to bring the pole either on the south or north pole, whichever is nearer. Suppose the pole coincide at south pole. Taking the centre at the south pole, an arc is drawn corresponding to the θ. Now the pole is brought to its original point by back rotation with respect to the axis perpendicular to the projection and coincides at the centre of the Wulff net first and then the E-W axis by the same number of degree by which it was rotated before (θ). The arc containing the new position of these points is traced, which in turn will be at the required number of degrees from the zone axis. The procedure is shown in Fig. 3.5. This process is carried out for the other zone axis also. The intersection of the two small arcs fixes the location of desired growth direction. Now the angle between this axis and the centre is measured by aligning the two poles to lie along the equator. In term of this angle, the orientation of the crystal is expressed.

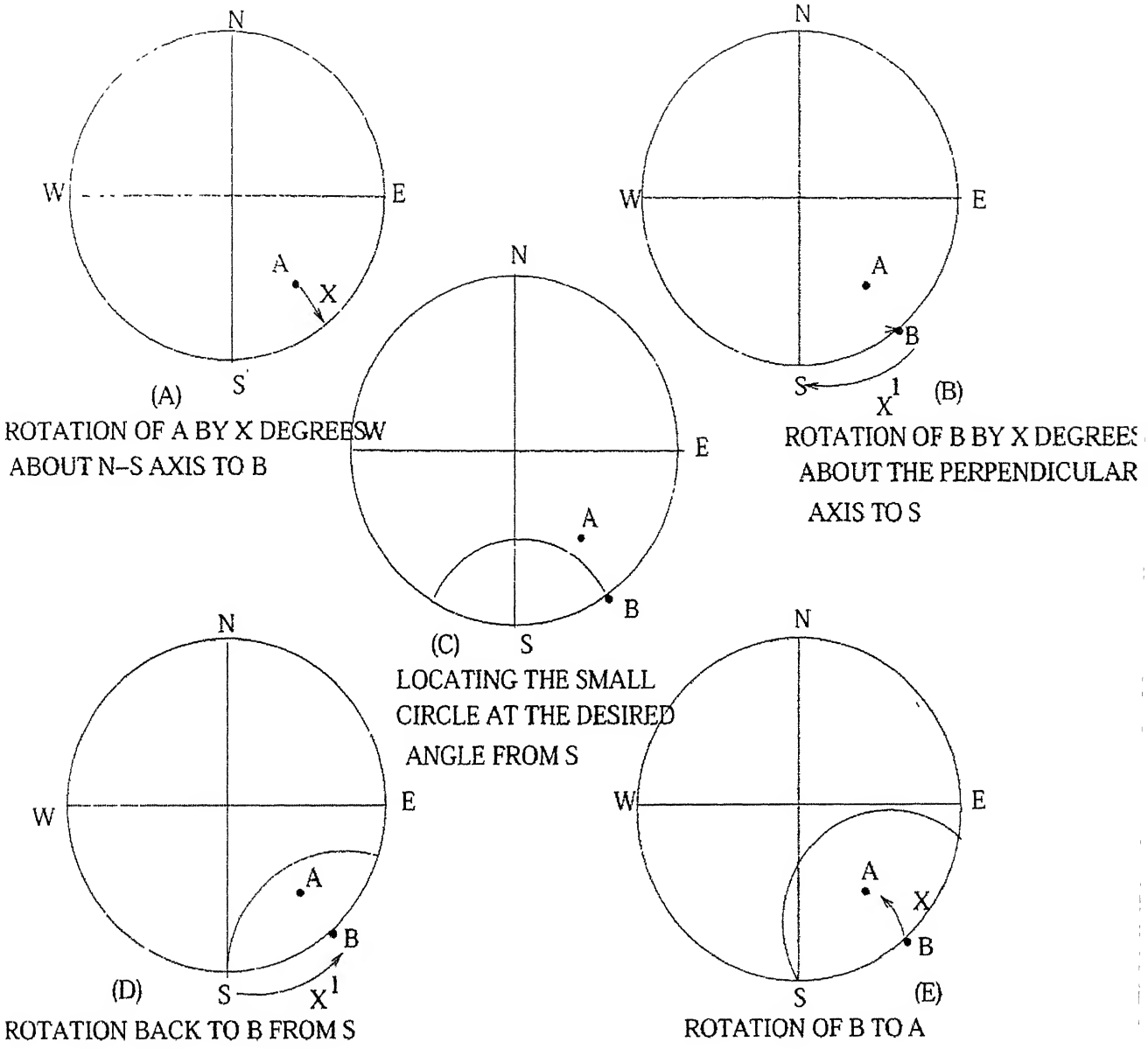

Figure 3.5 Determination of growth direction

CHAPTER 4

RESULTS AND DISCUSSION

A computer program developed in 'C' language for indexing of Laue back reflection patterns specifically for body centered tetragonal system (like Sn-Bi) by Ranjan [6] has been used in the present work. Laue back reflection patterns of Sn-Bi alloys of 2 wt% and 6wt% Bi prepared by directional solidification with different freezing rate (as mentioned in Table3.1), have been recorded using continuous X-rays from a copper target (operating accelerating voltage 30 kV and beam current 20 mA) on a photographic sheet film held at 3 cm away. Their traces have been shown schematically in Fig. 4.1-4.4 by placing the film upside down with identification numbers assigned to Laue spots, x–y axes and cut in the film for determining the side used during exposure. The x and y coordinates of Laue spots and their corresponding angular distances (γ and δ) are listed in tables 4.1–4.4 for samples 1–4, respectively. The location of each Laue spot on the stereographic projection for the four samples under study are shown in Fig. 4.5–4.8. Those Laue spots, which fall on a great circle (or particular hyperbola on the photographic film) in the stereographic projection correspond to a zone and indicated by letter code (A, B, C.....) in Fig. 4.5–4.8. By feeding the input data, viz , x and y coordinates of Laue spots falling on great circles of the stereographic projection, specimen to film distance as 3 cm, lattice parameters for Sn–Bi system (belonging to body centered tetragonal) as a = b = 5.8190 $\overset{0}{A}$, c = 3.1749 $\overset{0}{A}$ in the computer, the program was run to determine the indices of each pole (or Laue spots). Subsequently, zone indices (u v w) were determined using the equation hu + kv + lw = 0, where h k l represent the indices of Laue spots. Another test of three Laue spots if lying on a zone is to see the determinant of their indices is zero. This process yield results as summarized in Table 4.5–4.8

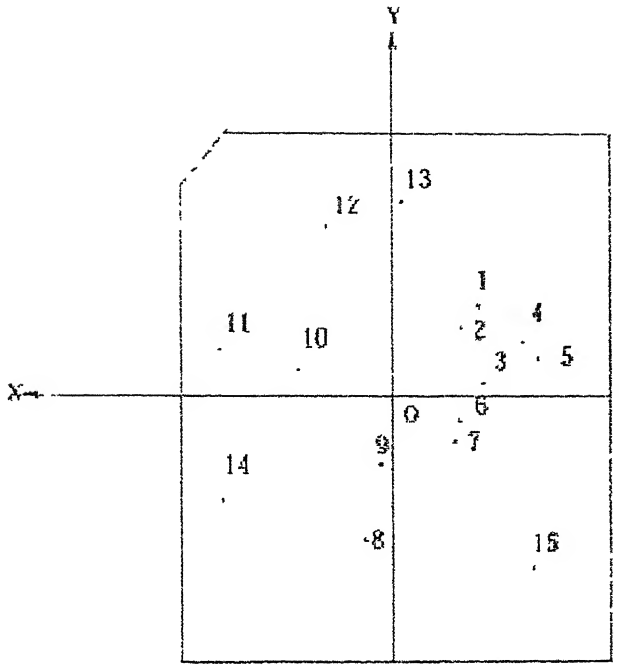

Figure 4.1 Laue back reflection pattern of sample 1 (Sn-2wt%Bi, 127.3 μm/s)

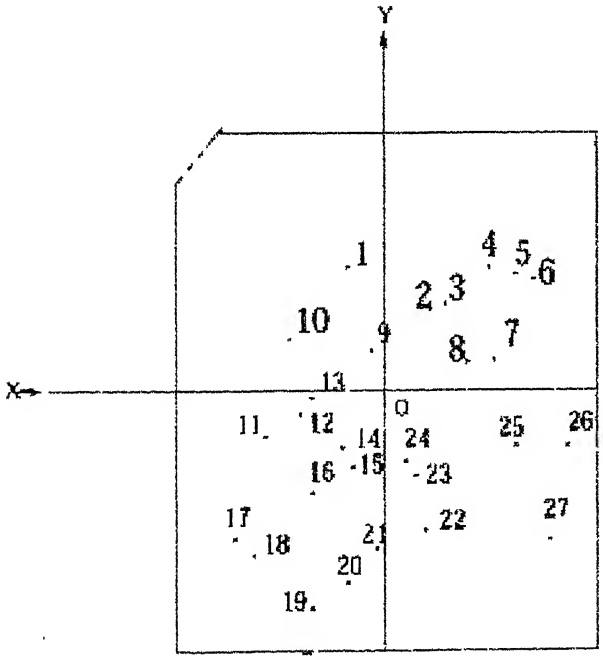

Figure 4.2 Laue back reflection pattern of sample 2 (Sn-2wt%Bi, 68.39 μm/s)

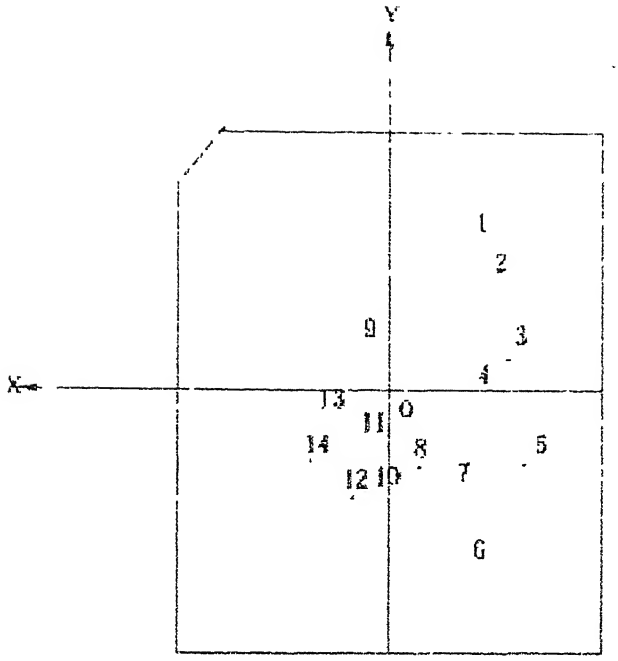

Figure 4.3 Laue back reflection pattern of sample 3 (Sn-6wt%Bi, 68 39 μm/s)

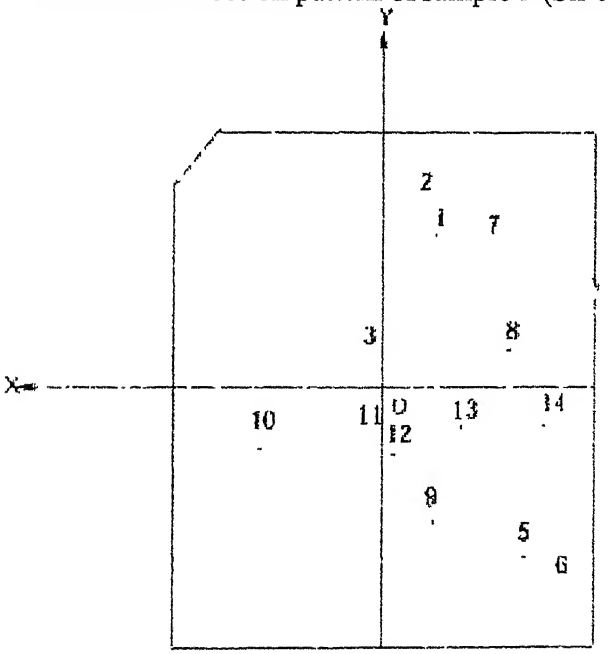

Figure 4.4 Laue back reflection pattern of sample 4 (Sn-2wt%Bi, 51.02 μm/s)

Table 4.1 The x- and y- coordinates of Laue spots and their corresponding angular distances (γ and δ) as read on the Greninger Chart for sample 1 (Sn-2 wt% Bi, 127.38 μm/sec.)

Spot No.	Coordinates (cm)		Angular distance (degree)	
	x	y	γ	δ
1	2 80	-3.80	14	-12
2	-1.1	1 3	12	-10
3	-1.65	0.25	3	-15
4	-3 5	1.10	8	-24
5	-3.4	0.80	6	-24
6	-1.10	-0.40	-4	-10
7	-1.00	-1.30	-8	-10
8	0.80	-2.60	-17	6
9	0.40	-1.20	-12	4
10	2.60	-3.00	4	16
11	3 45	1.90	14	23
12	1 00	3 00	23	10
13	-0.05	3.75	26	-1
14	3.40	1.90	-14	23
15	-3.00	-2.40	-18	-20

Relation between coordinates of spots (x and y) and angular distances (γ and δ):

$$\tan\mu = \frac{\tan\delta}{\sin\gamma}, \qquad \tan\sigma = \frac{\tan\delta}{\sin\mu\cos\gamma}$$

$x = d \tan 2\sigma \sin\mu$ cm, $y = d \tan 2\sigma \cos\mu$ cm

Where d is the specimen to film distance.

Table 4.2 The x- and y- coordinates of Laue spots and their corresponding angular distances (γ and δ) as read on the Greninger Chart for sample 2 (Sn-2 wt% Bi, 68.39 μm/sec.)

Spot No.	Coordinates (cm)		Angular distance (degree)	
	x	y	γ	δ
1	0 55	1 60	19	6
2	-1.0	1 90	16	-8
3	-1.20	2 00	17	-10
4	-1.65	2 35	19	-13
5	-1.40	-0 75	18	-17
6	-1.16	2.35	17	-18
7	-1.90	0.65	6	-14
8	-1 40	0.65	6	-12
9	0.30	0.80	8	2
10	2.10	1.10	10	17
11	1.75	-0.60	-6	20
12	1.45	-0 30	-3	17
13	1.35	-0.15	-1	14
14	0.75	-0.90	-10	9
15	0.70	-1.10	-12	8
16	1.35	-1.35	-15	13
17	1.70	-1 65	-19	19
18	1.55	-1.90	-21	17
19	1.00	-1.45	-27	10
20	0.55	-2 40	-26	6
21	0.35	-2.20	-23	1
22	-0.45	-1.80	-20	-5
23	-0.35	-1 25	-14	-4
24	-0.20	-1.10	-12	-2
25	-1.9	-0.65	-8	-29

Table 4.3 The x- and y- coordinates of Laue spots and their corresponding angular distances (γ and δ) as read on the Greninger Chart for sample 3 (Sn-6 wt% Bi, 68.39 μm/sec.)

	Coordinates (cm)		Angular distance (degrees)	
Spot No.	x	y	γ	δ
1	-1.45	3.00	22	-10
2	-1.65	2.55	20	-12
3	-2.05	0.75	7	-17
4	-1.85	0.15	2	-16
5	-3.25	-1 40	-10	-24
6	-1.50	-2 50	-20	-12
7	-1.40	-1.80	-15	-11
8	-0.40	-1.40	-12	-4
9	0.55	0.75	8	6
10	0.25	-1.80	-16	2
11	0.75	-0.95	-9	7
12	0.70	-1.80	-16	6
13	1.80	-0.55	-06	16
14	1.70	-1.15	-10	14

Table 4.4 The x- and y- coordinates of Laue spots and their corresponding angular distances (γ and δ) as read on the Greninger Chart for sample 4 (Sn-2 wt% Bi, 51.02 μm/sec.)

Spot No.	Coordinates (cm)		Angular distance (degree)	
	x	y	γ	δ
1	-0.85	3.05	28	-8
2	-0.85	3.50	24	-6
3	0.45	0.70	8	6
4	-0.90	-2 65	-24	-8
5	-2.60	-3 20	-24	-18
6	-3 10	-3.85	-26	-20
7	-2.00	2.75	20	-14
8	-2.25	0.80	8	-20
9	-4.00	1.55	14	-28
10	2.65	-1.25	-10	20
11	0.55	-0.95	-10	6
12	-0.10	-1.25	-14	0
13	-1.45	-0.80	-7	-14
14	-2.50	-0.70	-6	-29

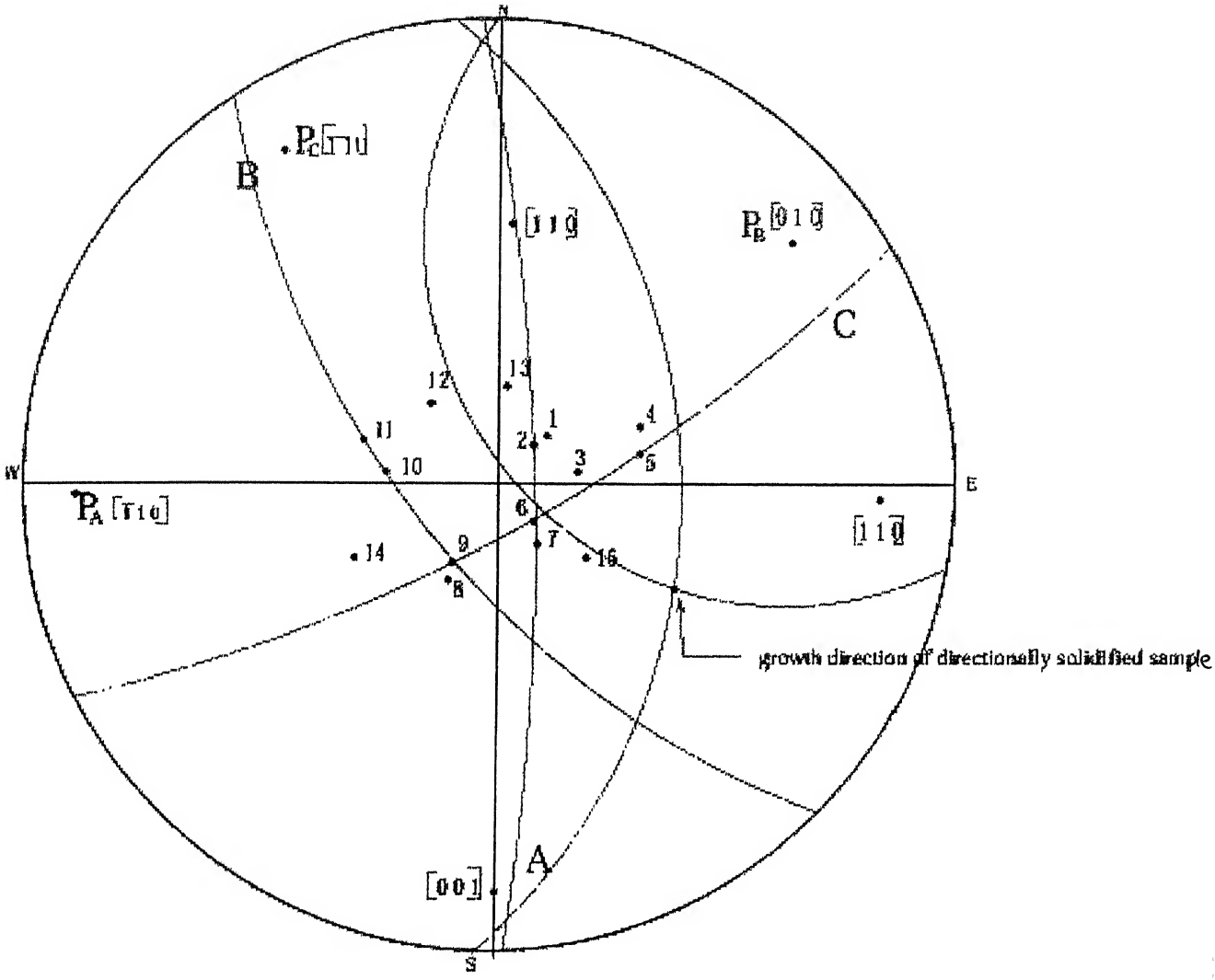

Figure 4.5 Stereographic projection of sample 1 (Sn-2wt%Bi, 127.3 μm/s) where P_A, P_B, and P_C are the poles of zone A, B, and C.

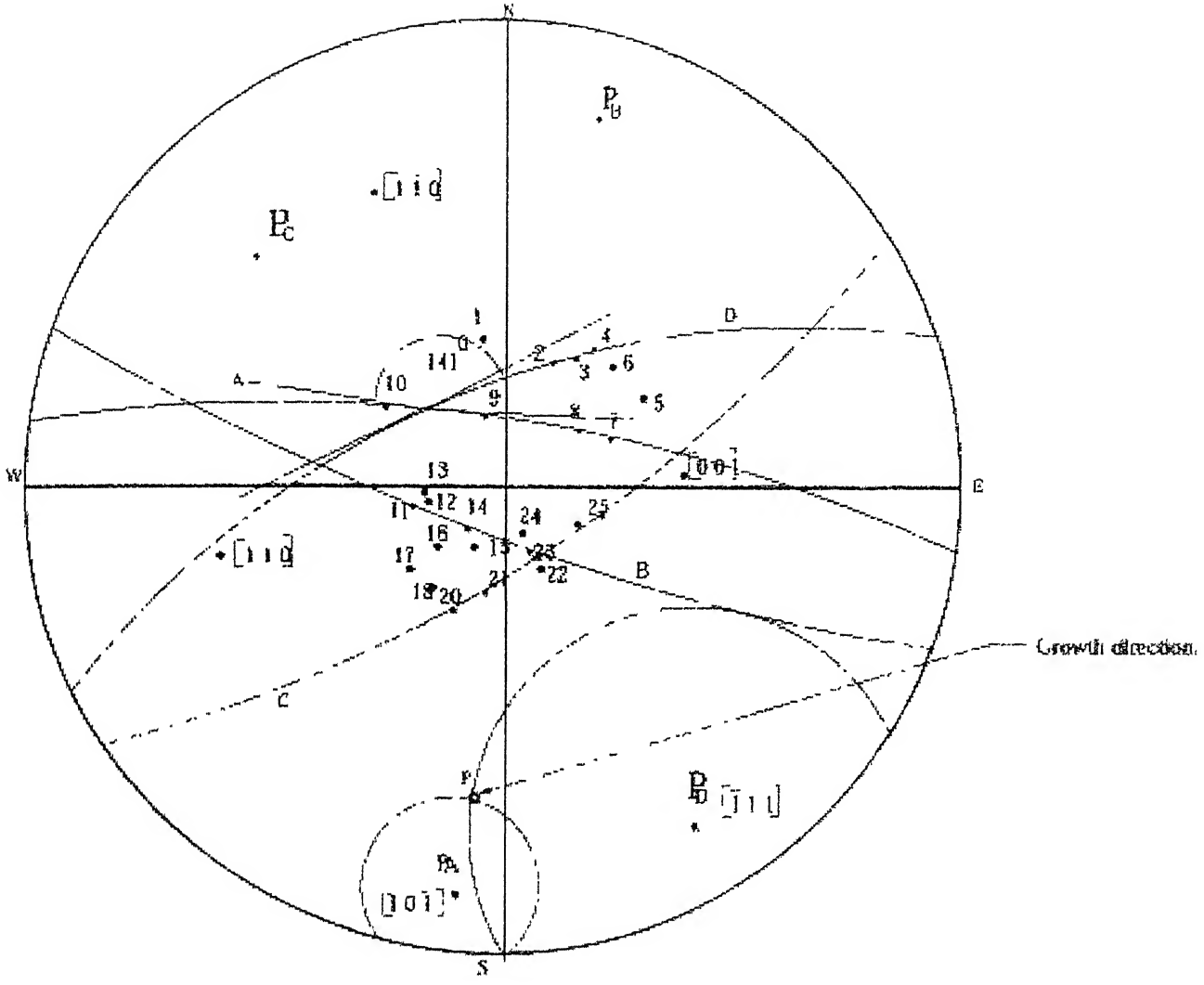

Figure 4.6 Stereographic projection of sample 2 (Sn-2wt%Bi, 68.39 μm/s)

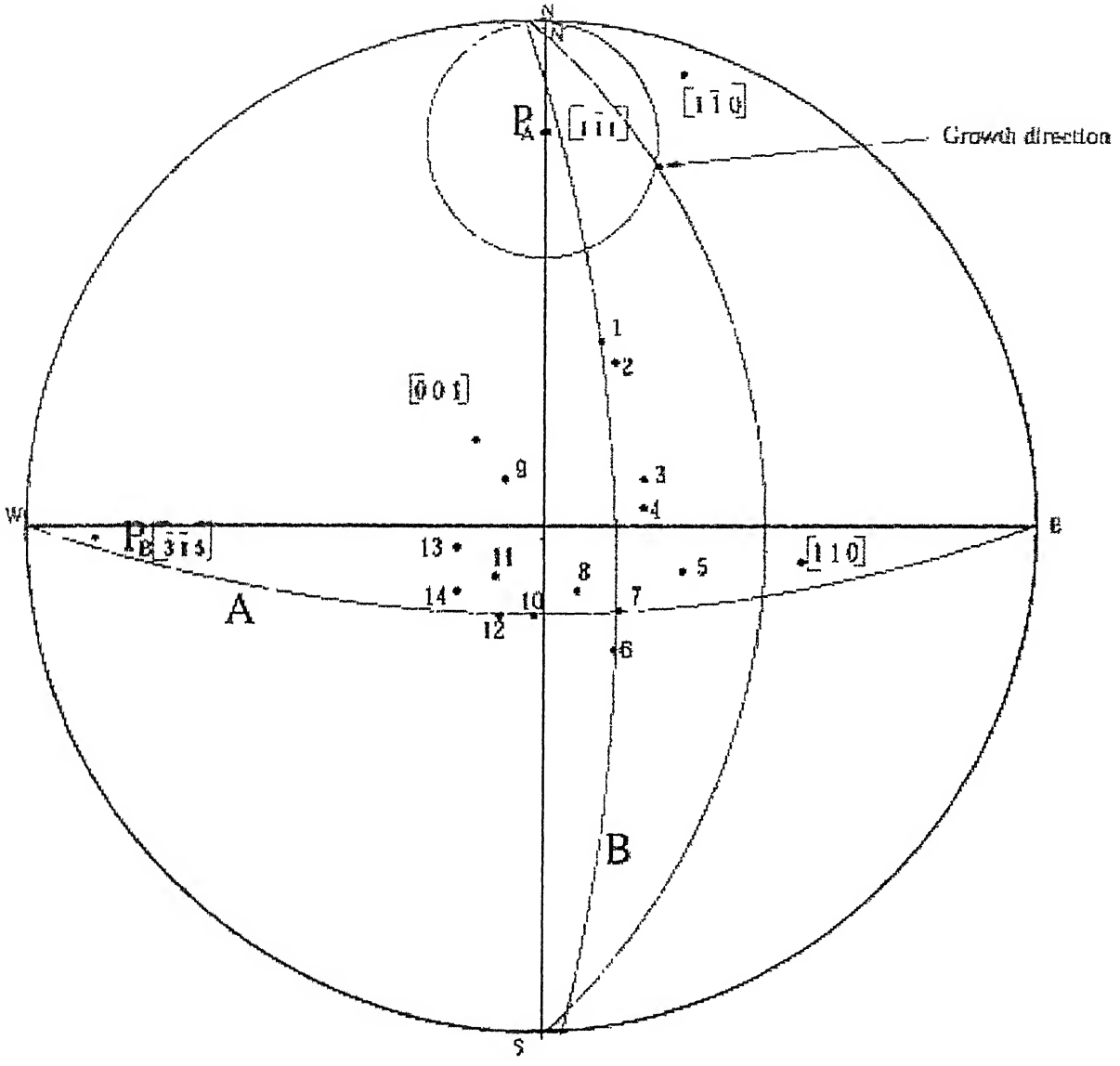

Figure 4.7 Stereographic projection of sample 3 (Sn-6wt%Bi, 68.39 μm/s)

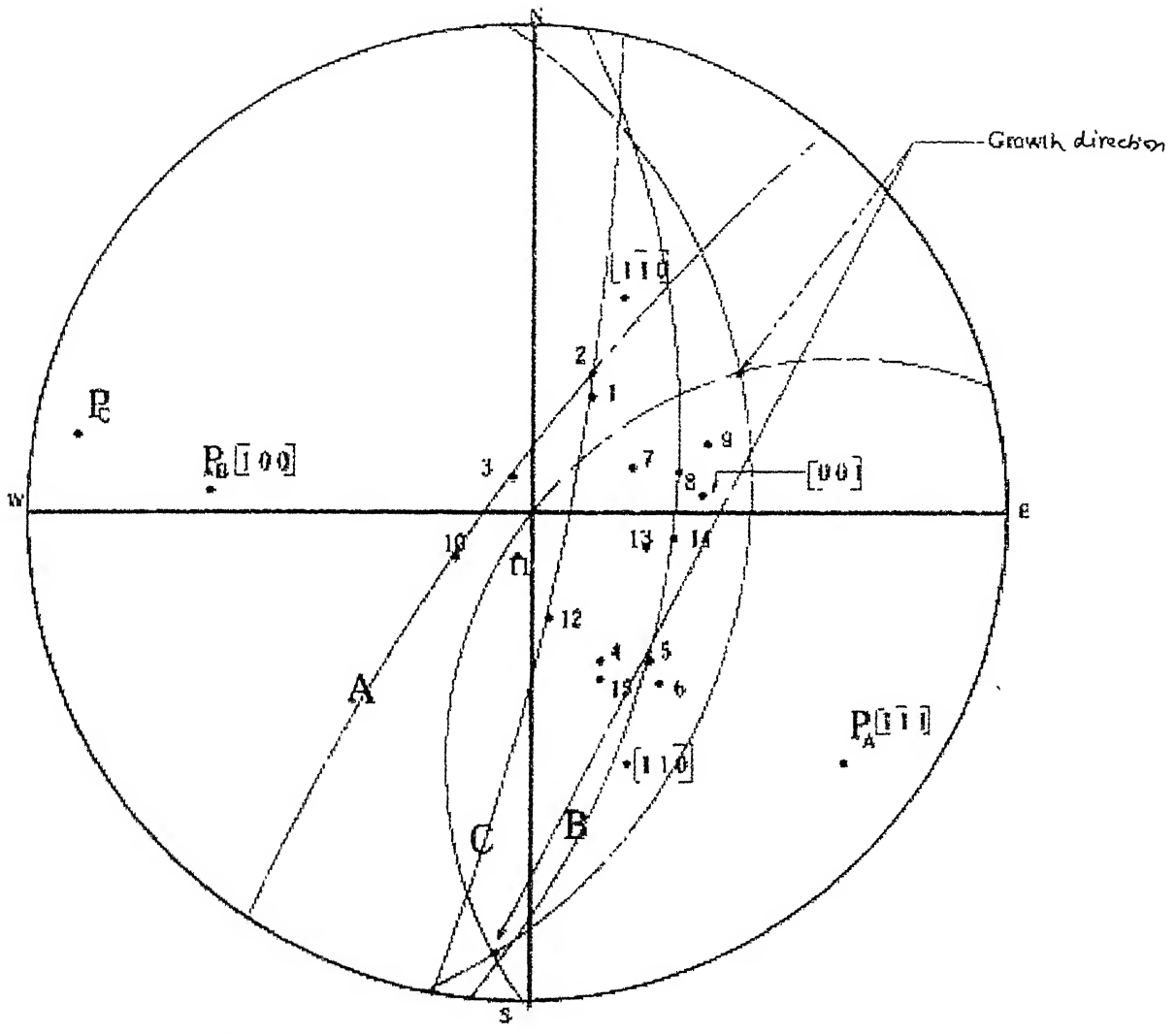

Figure 4.8 Stereographic projection of sample 4 (Sn-2wt%Bi, 51.02 μm/s)

Table 4.5 Indices of Laue spots and zone axes of sample 1 (Sn-2wt%Bi, 127.3 μm/s)

Laue spot No.	h k l	Zone	Angle between zones (degree)		Difference
			Theoretical*	Experimental+	
2	$0\ \bar{3}\ 1$	[3 1 3] for spots 2, 6, 7 & [0 $\bar{1}$ $\bar{2}$] for spots 5, 6, 9	121.9	121 0± 1	0.9∓1
5	$1\ \bar{6}\ 3$				
6	$\bar{1}\ \bar{6}\ 3$				
7	$\bar{1}\ \bar{3}\ 2$				
9	$\bar{1}\ \bar{2}\ 1$				

* Theoretical angle is calculated by computer program.

\+ Experimental angle is measured on stereographic projection

Table 4.6 Indices of Laue spots and zone axes of sample 2 (Sn-2wt%Bi, 68.39 μm/s)

Laue spot No.	h k l	Zone	Angle between zones (degree)		Difference
			Theoretical	Experimental	
2	$\bar{5}\,\bar{1}\,\bar{4}$	$[\bar{1}\ 1\ 1]$ for spots 2, 3, 4 & $[1\ 0\ \bar{1}]$ for spots 7, 8, 9	138.6	141 0± 1	2.4± 1
3	$\bar{4}\,\bar{1}\,\bar{3}$				
4	$\bar{6}\,\bar{2}\,\bar{4}$				
7	$\bar{6}\,\bar{4}\,\bar{6}$				
8	$\bar{4}\,\bar{2}\,\bar{4}$				
9	$\bar{6}\,0\,\bar{6}$				

Table 4.7 Indices of Laue spots and zone axes of sample 3 (Sn-6wt%Bi, 68.39 μm/s)

Laue spot No.	h k l	Zone	Angle between zones (degree)		Difference
			Theoretical	Experimental	
1	$\bar{6}\,\bar{2}\,\bar{4}$	$[\bar{3}\ \bar{1}\ 5]$ for 1, 6, 7 & $[1\ \bar{1}\ 1]$ for 7,10, 12	94.6	92 0±1	2.6∓1
6	$\bar{3}\,\bar{6}\,\bar{3}$				
7	$\bar{2}\,\bar{4}\,\bar{2}$				
10	2 6 4				
12	1 4 3				

Table 4.8 Indices of Laue spots and zone axes of sample 4 (Sn-2wt%Bi, 51.02 μm/s)

Laue spot No.	h k l	Zone	Angle between zones (degree)		Difference
			Theoretical	Experimental	
2	$\bar{1}3\bar{4}$	[1 $\bar{1}$ $\bar{1}$] for 2, 3, 10 & [1 0 0] for 5, 8, 14	48.7	47.0 ± 1	1 7∓1
3	$\bar{2}1\bar{3}$				
5	$0\bar{2}\bar{4}$				
8	$01\bar{5}$				
10	$\bar{5}\bar{1}\bar{4}$				
14	$0\bar{1}\bar{5}$				

4.1 Determination of growth direction

The possible growth directions for Sn–Bi system are [1 1 0], [1 $\bar{1}$ 0], and [0 0 1]. While major growth of primary dendrite takes place along [1 1 0] and [1 $\bar{1}$ 0], minor growth occurs along [0 0 1] in Sn-Bi alloys [3–5]. These directions are located on the stereographic projections shown in Fig. 4.5–4.8. Location of these directions is determined on the stereographic net using the expected angles between axis and the growth directions.

The growth direction is determined by measuring the angle between the zone axis and the stereographic projection. The angles between various zone axes and the centre of the stereographic projection (or incident X-ray beam direction) are given in Table 4.9.

Also the angles between reported growth directions in Sn-Bi system (viz [1 1 0], [1 $\bar{1}$ 0] and [0 0 1] and the ingot axis (which is represented by the centre of stereographic projection) were measured by bringing both points on same circle. These are given in table 4.10 together with that found in the present work. By matching the angles, the growth direction (or ingot axis) can be found out. Accordingly, for sample 2 growth of directionally solidified Sn-Bi system occurs along [1 $\bar{1}$ 0]. But for sample 4, growth direction can be either [1 1 0] or [1 $\bar{1}$ 0]. There is no matching of angle for other samples, namely 1 and 3. So growth directions were independently determined, which were found [$\bar{2}$ 1 3] and [0 1 $\bar{1}$]

TABLE 4.9

Angles between zone axes and incident X-ray beam (i.e. ingot axis) or centre of stereographic projection

Sample (Sn-Bi)			Zone Axis corresponding to hyperbola in Laue photograph	Angle between the zone axis and incident X-ray beam (degree)
No.	wt%Bi	Rate* (μm/s)		
1	2	127.3	$[\bar{1}\ 1\ 0]$ [0 1 0]	80 80
2	2	68.39	[1 0 1] $[\bar{1}\ 1\ 1]$	68 80
3	6	68.39	$[\bar{3}\ \bar{1}\ 1]$ $[1\ \bar{1}\ 1]$	88 82
4	2	51.02	$[1\ \bar{1}\ \bar{1}]$ [1 0 0]	80 70

* Freezing rate

Table 4.10

Measured angles between ingot axis (i.e. the centre of stereographic projection) and the growth directions in Sn-Bi system

Sample (Sn-Bi)			Angle (in degrees) with the growth direction			
No.	wt%Bi	Rate*	[1 1 0]	[1 $\bar{1}$ 0]	[0 0 1]	Found in the present work
1	2	127.3	60	80	80	40
2	2	68.39	50	64	32	68
3	6	68.39	42	82	18	70
4	2	51.02	54	50	24	52

* Freezing rate (μm/s)

4.2 Discussion

The usual solidification process requires liquid-solid interface to be planar at least locally. This is achieved by sufficiently high thermal gradient in the liquid (G) and low growth/freezing rate (R). However, a solute rich boundary layer builds up in front of a solidifying planar interface with time and cause instability of the plane front [26]. In this situation, liquid composition decreases (causing liquidus temperature to increase) with increasing distance from the interface; the maximum being at the interface itself As a consequence, a protuberance may form on the flat interface. At this stage, the temperature of the liquid just at the interface is less than its equilibrium liquidus temperature. It is therefore supercooled and is termed as constitutional supercooling (origin being change in composition and not temperature)

According to the constitutional supercooling criterion the interface is stable when [27]

$$\frac{G}{R} \geq -\frac{mC_0(1-k_0)}{k_0 D}$$

Where G is the temperature gradient at the interface, R is the freezing rate, m is the liquidus slope, C_0 is the average composition, k_0 is the equilibrium distribution coefficient and D is the diffusivity of solute in liquid The terms on the left hand side correspond to growth conditions whereas those on the right hand side are material and system parameters. Accordingly, constitutional supercooling may occur at (i) low temperature gradients (ii) fast growth rates, (iii) steep liquidus lines i.e. large m, (iv) high average composition C_0, (v) low diffusivity, D and (vi) low k_0 for $k_0 < 1$. In the present case of Sn-Bi alloy, constitutional supercooling may result with increase in the freezing rate and/or increase in bismuth content. The nature of the interface (i.e., turning planar to cellular, extended cell caps type, cellular-dendrites, etc.) depending on the degree of supercooling prevailing during the solidification process.

4.2.1 Effect of freezing rate

Samples 1, 2, and 4 having the same composition (Sn-2wt%Bi) but are produced with different freezing rates viz., 127.3 μm/s, 68.39 μm/s and 51.02 μm/s, respectively. For sample 2, grow ı occurs along [1 $\bar{1}$ 0] whereas for sample 4, preferred growth direction is [1 $\bar{1}$ 0] or [1 1 0] or both. These findings correspond to low freezing rate conditions and match well with the reported growth directions for Sn-Bi system [3-5]. In case of sample 1, which is produced at higher freezing rate, the growth direction is of higher indices [$\bar{2}$ 1 3].

At low freezing rate regular cells form perpendicular to the liquid-solid interface regardless of the crystal orientation. The resulting cell is of circular cross section. With ıncrease in freezing rate, crystallographic effect begin to exert an influence and the cell-growth occurs along the preferred direction with deviation in its previously circular geometry to flanged structure. Further, increase ın freezing rate, cross structure first becomes more apparent and then serrations begin to appear in the flanges of the cross,

i.e., secondary dendrite arms become discernible [28] The overall effect may be such that the growth assumes altogether a different crystallographic direction.

The total free energy for solidification mainly consists of the free energies for nucleation, growth, and creating the interface. The system grows along the direction requiring the minimum free energy. At high freezing rate, large interface area gets generated because of the prevailing instability and so associated interfacial energy will also be large. Therefore, energy available for the growth becomes less as some energy got consumed during creation of the interface. Thus the growing direction gets deviated.

4.2.2 Effect of composition

Samples 2 and 3 are produced at the same freezing rate (68.39 μm/s), but, have different compositions viz., Sn-2wt%Bi and Sn-6wt%Bi, respectively. The growth direction in case of sample 2 is [1 $\bar{1}$ 0] which matched well with reported growth direction for Sn-Bi system [3-5] In case of sample 3, which has more Bi content, growth occurs along an altogether a different direction i.e. [0 1 $\bar{1}$]. At high bismuth content, constitutional supercooling may result and form protrusion at the interface, which may alter the shape of the protrusion. This is perhaps the reason for deviation in the growth direction in 6wt%Bi alloy.

CHAPTER 5

CONCLUSIONS

1. The preferred growth directions were determined in Sn-Bi alloys of compositions 2wt% and 6wt% Bi produced by directional solidification at freezing rates of 51.02 μm/s, 68.39 μm/s, and 127.3 μm/s by Laue X-ray back reflection method.
2. Electropolishing of samples at 34 volts and current of 1.39 A in solution of 70% (v) ethanol (absolute), 12% (v) distilled water, 10% (v) 2-butoxyethanol and 8% (v) perchloric acid (70%) of specific gravity 1.67 solution at 18^0 C and subsequent etching in $K_2Cr_2O_7$ solution were found to be ideal for observing the microstructure and identification of the location the largest grain
3. For 2wt% Bi alloys at low freezing rate, the preferred growth directions found are of low indices i.e , [1 $\bar{1}$ 0] and/or [1 1 0]. However, at higher freezing rate, the growth occurs along higher indices i.e., [$\bar{2}$ 1 3]. The deviation is attributed to (i) the diversion of the free energy available in creating large interface and (ii) the appearance of serrations in the flanges of the cross section of the cells at higher freezing rates.
4. The increase in bismuth content leads to altogether a different growth direction in Sn-Bi alloys. While in 2wt%Bi alloy, preferred growth occurs along [1 $\bar{1}$ 0], the corresponding direction in 6wt% Bi alloys is [0 1 $\bar{1}$]. The possible reason for deviation could be the constitutional supercooling at higher Bi content leading to protrusion at the interface.

CHAPTER 6

REFERENCES

1. V. Raghavan, "Physical metallurgy, princilpes and practice", 12th edition, Prentice Hall, New Delhi, 2000.
2. W. H. Huang, J. H. Christensen, and R. J. Block "A computer technique for the solution of Laue back reflection patterns of cubic crystals, part I", Met. Trans. A, 2 (1971) 1367.
3. F. Weinberg and B. Chalmers, "Dendrite growth in metals", Canadian Journal of Physics, 30 (1952) 488.
4. P. J. Aheran and M. C. Fleming, "Dendrite morphology of a Sn-Bi alloy", Trans. of Met. Soc. of AIME, 239 (1967) 1590.
5 G. F. Boiling, J. J. Kramer, and W. A. Tiller, "Preferred orientations of high purity zinc and tin", Trans. of Met. Soc. of AIME, 227 (1963) 1453.
6. A. Ranjan, "Development of computer code in 'C' for indexing of Laue back reflection patterns from directionally solidified Sn-Bi alloys" M.Tech. Thesis, I.I.T Kanpur, May 2000.
7. P. Ravi Kumar, "The effect of changes in freezing rates on primary dendrite spacing in directionally solidified dilute alloys of Bi in Sn", M. Tech. Thesis, I.I.T. Kanpur, August 1991.
8 R. Trivedi, V. Seetharaman, and M. A. Eshelman, "The effect of interface kinetics anisotropy on the growth direction of cellular microstructures", Met. Trans. A, 22 (1991) 585.
9. A. Larrea, L. Contreras, R. I. Merino, J. Llorca, and V. M. Orera, "Microstructure and physical properties of CaF_2 – MgO eutectics produced by the Bridgman method", J. Mater. Res., 15 (2000) 1314

10 M. A. Martorano and J. D. T. Capochhi, "Effects of processing varibles on the microsegregation of directionally cast samples", Met & Met. Tran. A, 31 (2000) 3137.

11 B. D. Cullity, "Element of X-ray diffraction", 2nd edition Addison – Wesley, Reading, Massachusetts, 1978.

12. J. H. Christensen, W. H. Huang, and R. J. Block, "A computer technique for the solution of Laue back reflection pattern of cubic crystals, part II", Met. Trans. A, 2 (1971) 2295.

13. D. T. Camp and J. A. Clum, "Computer program for calculating interplanar angles and indexing Laue back reflection data in an arbitrary crystal system", Trans. of Met. Soc. of AIME, 236 (1966) 1752.

14 C. A. Cornelius, "A simple program for the orientation of single crystal of any structure using Laue back reflection X ray photographs", Acta Cryst. A31 (1981) 430.

15 J. Laugier, "An interactive program for the interpretation and simulation of Laue patterns", J. Appl. Cryst. 16 (1983) 281.

16 P. Riquet and R. Bonnet, (1979), J. Appl. Cryst., 12 (1979) 39.

17 H V. Hart and E. A. Rietman, "Indecing asymmetrical Laue photographs: application to echinoid calcite", J. Appl. Cryst., 15 (1982) 126.

18 P. S. Kumar and V. Bansal, "Computer aided indexing of Laue back reflection patterns of body centre tetragonal crystals", Trans. of Indian Institute of Metals, 48 (1995) 491.

19 B. S. Chandrashekhar and B. W. Veal, "Crystallographic angles in tetragonal crystal: β - tin and indium", Trans. of the Met. Soc. of AIME, 221 (1961) 202.

20 R. E. Frounfelker and W. M. Hirthe, "Crystallographic data for the tetragonal crystal", Trans. of the Met. Soc. of AIME, 224 (1962) 196.

21 J. A. Lee and G. V. Raynor, "The lattice spacing of binary tin rich alloys", Proc. Phy. Soc , B671(954) 737.

22 R. Kumar, "The effect of changes in freezing rates on primary dendrite spacing in directionally solidified dilute alloys of bismuth in tin", M.Tech. Thesis, I.I.T. Kanpur, August 1991.

23 N. Das, "Morphology and dendrite spacing of Sn-Bi alloys", M.Tech. Thesis, I.I.T. Kanpur, July 1984

24 Metal Handbook, 9th edition, 9 (1978) 22.

25 Buehler Ltd, Metallurgical apparatus 20, Greenwood Evanston, 111, U.S A. 60204.

26 M. C. Flemings, "Solidification processing", McGraw-Hill, New Delhi, 1974.

27 G. J. Davies, " Solidification and casting", Applied science publishers, 1973.

28 M. C. Flemings, " Solidification processing", McGraw-Hill, New Delhi, (1974) 73.